UCRL 3320

UNIVERSITY OF CALIFORNIA

Radiation Laboratory

BERKELEY, CALIFORNIA

DISCLAIMER

UCRL-3320

UNIVERSITY OF CALIFORNIA
Radiation Laboratory
Berkeley, California

Contract No. W-7405-eng-48

NEUTRON YIELDS FROM THICK TARGETS BOMBARDED BY 18- AND 32-Mev PROTONS

George Patrick Millburn

(Thesis)

February 21, 1956

Printed for the U. S. Atomic Energy Commission

NEUTRON YIELDS FROM THICK TARGETS BOMBARDED BY 18- AND 32-Mev PROTONS

Contents

NEUTRON YIELDS FROM THICK TARGETS BOMBARDED BY 18- AND 32-Mev PROTONS

George Patrick Millburn

Radiation Laboratory
University of California
Berkeley, California

February 21, 1956

ABSTRACT

Neutron yields from thick targets bombarded by 32- and 18-Mev protons were measured for 59 elements and compounds. Also, for 23 metallic elements yields were measured from targets thick enough to degrade the proton energy from 32 to 18 Mev. The neutrons were detected by counting the Mn^{56} activity produced by neutron capture in $MnSO_4$ solution contained in a 3-by-3-ft tank that surrounded the targets. The efficiency of the neutron-detection system was determined with a calibrated Ra-α-Be source. For all three energy intervals, the neutron yields increased abruptly by a factor of 2 at Z = 20 and Z = 30, and Ni had a yield 1/3 that of neighboring elements.

When analyzed in terms of the average number of neutrons per nuclear interaction, $\overline{N}$, the data may be examined in terms of the statistical theory of nuclear reactions. The increase in $\overline{N}$ with energy agreed with a rough estimate from the theory, but values of $\overline{N}$ were 30% to 60% lower than the predicted values for $Z < 40$. $\overline{N}$ showed a close correlation with $\theta_t = (N - Z)/A$ of the target nuclei, and a term proportional to $\theta_t - \theta_c$ added to the exponent in the usual expression for the probability of neutron emission from a compound nucleus gave fair agreement between measured and calculated values. Some such term was found to be necessary in order to obtain correct values of $\overline{N}$ and to reproduce the observed discontinuities.

I. INTRODUCTION

The production of neutrons in nuclear reactions has been of interest for more than 20 years, first from reactions produced by naturally occurring α particles,[1] and later from reactions of accelerated particles.[2] The interest in neutron sources today is confined largely to the production of monoenergetic beams, and general total-production measurements are of relatively little concern. Nevertheless, data on total neutron production in nuclear reactions may be used to check the predictions of the statistical theory of nuclear reactions,[3] and are needed in order to design shielding for particle accelerators.

The data are valuable in indicating nuclei whose neutron emission is anomalous, and form the first step in a systematic survey of proton reactions in this energy region that lead to neutron emission. In this connection the discontinuities in neutron yields observed at $Z = 20$, $Z = 30$, and for Ni are of special interest.

Total neutron production by protons has not heretofore been thoroughly investigated; most of the work has been with deuterons and alpha particles.[4, 5] In recent years the total neutron production by high-energy protons in thick targets has been measured for 12-Mev,[6] 340-Mev,[7] and 400-Mev[8] protons as well as for other particles[6, 7] by the technique used in this experiment. The work reported here is much more comprehensive in surveying the neutron production throughout the periodic table, and extends the measurements to a new energy region. Cohen has recently published similar data for nine elements bombarded by 21.5-Mev protons,[9] but his measurements are subject to greater uncertainties in the total yield.

In the work to be described, the neutron production of 32-Mev protons bombarding thick targets of 59 elements and three separated isotopes, and of 18-Mev protons bombarding thick targets of 49 elements has been measured. In addition the neutron production of protons with energy between 18 and 32 Mev has been measured for 23 elements. The source of the protons was the 32-Mev proton linear accelerator,[10] and the incident proton flux was measured by placing the targets in a

Faraday cup. The neutrons were detected by surrounding the targets with a solution of $MnSO_4$; after the neutrons were thermalized by collisions with the hydrogen atoms, a fraction was captured by Mn^{55} to form radioactive Mn, ^{56} and the activity of the solution was determined with Geiger counters immersed in a sample of the solution. The detection system was calibrated against a standard Ra-α-Be source.[11]

The $MnSO_4$ tank method is probably the most accurate one available for the measurement of total neutron production. The major limitation is the accuracy with which neutron sources are calibrated. Although a great difference between the energy spectra of the source and of the target could lead to errors in the measurement, this limitation is not important except for very high-energy neutrons.

In the energy region under consideration, nuclear reactions are usually analyzed in terms of the statistical theory developed by Weisskopf[3] and based in part on the concept of a compound nucleus.[12] Even though it is now recognized that other types of reactions may be more important than the compound nucleus, the first step in our analysis begins with the statistical theory because it is the only theory sufficiently well developed to permit detailed calculations. According to this theory, a nuclear reaction such as $X + p \rightarrow C \rightarrow Y + n$ may be thought of as occurring in two steps: first the target nucleus X and the incident particle (here chosen to be a proton for definiteness) form a compound nucleus C, and second the compound nucleus C decays to the residual nucleus Y and the outgoing particle (here chosen as a neutron for definiteness). The cross section $\sigma(p, n)$ for the over-all reactions may then be separated into two parts:

$$\sigma(p, n) = \sigma_C(E)\eta_n(E), \qquad (1)$$

where $\sigma_C(E)$ is the cross section for the formation of a compound nucleus by a proton of kinetic energy E and $\eta_n(E)$ is the probability that the compound nucleus decays by the emission of a neutron. The two factors of Eq. (1) may be further separated:

$$\sigma_C(E) = S(E)\xi(E) \tag{2}$$

where $S(E)$ is the cross section for reaching the nuclear surface and $\xi(E)$ is the probability of formation of a compound nucleus (sticking probability), and

$$\eta_n(E) = \frac{\Gamma_n(E)}{\Sigma\Gamma_b(E)}, \tag{3}$$

where $\Gamma_b(E)$ is proportional to the emission probability per unit time of a particle b and the sum is over all particles that can be emitted.

For energies greater than approximately 1 Mev, $\xi(E) = 1$, and tables of $\sigma_C(E)$ for various energies and nuclear radii may be found in Blatt and Weisskopf.[13] An approximation for protons that is quite simple and useful is

$$\sigma_C(E) = \pi(R + \lambda\!\!\!^{-})^2\left(1 - \frac{YR}{R + \lambda\!\!\!^{-}}\right). \tag{4}$$

Here $R = r_o A^{1/3}$ is the nuclear radius, $\lambda\!\!\!^{-} = \hbar/p$ is the de Broglie wavelength of a particle with momentum p, and $Y = [(Zze^2)/R]\,(1/E)$ is the ratio of the Coulomb barrier to the incident-particle energy E (our Y as defined is the inverse of Blatt's and Weisskopf's). The approximation is accurate to approximately 15% for $Y < 0.8$.[14] We have used the laboratory energy E because the Coulomb effect is small for light elements where the difference between laboratory and center-of-mass energy is important.

If we consider the emission from the compound nucleus of a particle b such that the residual nucleus is left in the definite state β with energy E_β, then we may write the width for the emission of b as the sum of the partial widths $\Gamma_{b\beta}^{(\ell)}$, where $\sqrt{\ell(\ell+1)}\,\hbar$ is the angular momentum of b,

$$\Gamma_b = \sum_{\beta,\ell} \Gamma_{b,\beta}^{(\ell)}, \tag{5}$$

and the energy with which b is emitted is $\epsilon_b = E - E_b - E_\beta$ where E_b is the binding energy of b. Now $\Gamma_{b\beta}^{(\ell)}$ refers to a process that is the reverse of the formation of a compound nucleus by particle b, with orbital angular momentum $\sqrt{\ell(\ell+1)}\,\hbar$, hitting the residual nucleus in the state β; from the cross section for that process, $\sigma_{b\beta}^{(\ell)}$, we may

calculate $\Gamma_{b\beta}^{(\ell)}$ by using the reciprocity theorem.[13] If Ω_{12} is the transition probability per unit time from a State 1 to a State 2, and ρ_2 is the density of states of State 2, then, from the theorem, we have

$$\Omega_{12}\rho_1 = \Omega_{21}\rho_2. \tag{6}$$

Now $\Omega = \Gamma/\hbar$, and here $\hbar\Omega_{12} = \Gamma_{b\beta}^{(\ell)}$, $\rho_1 = \omega_c$, $\Omega_{21} = v_b \sigma_{b\beta}^{(\ell)}$, and $\rho_2 = (2I + 1)(2S + 1)4\pi p^2 (2\pi\hbar)^{-3} v^{-1}$ for a free particle of spin S and residual nucleus of spin I. Then

$$\frac{\Gamma_{b\beta}^{(\ell)}}{\hbar}\,\omega_c(E) = v_b \sigma_{b\beta}^{(\ell)}\,\frac{(2I+1)(2S+1)P_b^{\,2}}{2\pi^2\hbar^3}\,\frac{1}{v_b},$$

or, since $p_b^{\,2} = 2m\epsilon_b$,

$$\Gamma_{b\beta}^{(\ell)} = \frac{(2S+1)(2I+1)}{\omega_C(E)}\,\frac{m\epsilon_b}{\hbar^2\pi^2}\,\sigma_{b\beta}^{(\ell)}(\epsilon_b). \tag{7}$$

If we substitute in Eq. (5), sum over ℓ and replace the sum over β by an integral, we have

$$\omega_C(E)\Gamma_b = \frac{m}{\hbar^2\pi^2}(2S+1)\int_0^{E-E_b} \epsilon\,\sigma_C(\epsilon)\,\omega_Y(E - E_b - \epsilon)\,d\epsilon, \tag{8}$$

where $\omega_Y(E)$ is the level density of the residual nucleus at an excitation energy E.

Then from Eqs. (3) and (8) we can calculate the probability of neutron emission from the compound nucleus, and hence the average number of neutrons emitted per nuclear interaction. We shall now show how we determined the latter quantity from the yield data.

Consider the production of neutrons by protons; we may define a cross section for the production of one neutron as

$$\sigma_{1n}(E) = \sigma(p, n) + \sigma(p, pn) + 2[\sigma(p, 2n) + \sigma(p, p2n)] + 3[\sigma(p, 3n) + \sigma(p, p3n)] + \ldots, \tag{9}$$

if we neglect those processes in which more than one proton is emitted and those which involve pickup reactions. In order to compare our results with theory, it is helpful to introduce the average number of neutrons per nuclear interaction, N(E), defined by

$$\sigma_{ln}(E) = \sigma_C(E)N(E). \tag{10}$$

Then the yield of neutrons produced by ϕ protons striking a target with range R (in g/cm^2) and atomic weight A is given by

$$y = \frac{\phi A_o}{A} \int_o^R \sigma_{ln} dx = \frac{\phi A_o}{A} \int_o^E \sigma_{ln} \frac{dx}{dE}\, dE, \tag{11}$$

where A_o is Avogadro's number. Now we may approximate the rate of energy loss by[15]

$$\frac{dE}{dx} = - CE^{-a}, \tag{12}$$

so we have

$$y = \frac{\phi A_o C}{A} \int_o^E \sigma_{ln} E^a dE = \frac{\phi A_o}{A} \overline{\sigma_{ln}} R, \tag{13}$$

or, from Eq. (10),

$$y = \frac{\phi A_o C}{A} \int_o^E \sigma_C(E)N(E)\, E^a dE = \frac{\phi A_o}{A} \overline{\sigma_C N}\, R. \tag{14}$$

Then from Eqs. (13) and (14) we have

$$\overline{\sigma_{ln}} = \overline{\sigma_C N} = \frac{y}{R} \frac{A}{\phi A_o}. \tag{15}$$

If we approximate* $\overline{\sigma_C N}$ by $\overline{\sigma_C}\ \overline{N}$, then we have

$$\overline{N} = \frac{\overline{\sigma_{ln}}}{\overline{\sigma_C}} = \frac{y}{R\overline{\sigma_C}} \frac{A}{\phi A_o}. \tag{16}$$

We use Eq. (4) to approximate $\sigma_C(E)$ in forming $\overline{\sigma_C}$:

$$\overline{\sigma_C} = \frac{1}{R} \int_B^E \sigma_C(E) \frac{dx}{dE}\, dE = \frac{1}{RC} \int_B^E \sigma_C(E) E^a dE, \tag{17}$$

where B is the Coulomb barrier of the nucleus. We can calculate $\overline{\sigma_C}$

---

* The approximation is satisfactory as long as $\sigma_C(E)$ is not rapidly changing; it begins to break down for the heavier nuclei for 18-Mev protons.

and we can measure $\overline{\sigma_{1n}}$, so that we can estimate the number of neutrons emitted per nuclear interaction when protons bombard thick targets.

After we have determined $\overline{N}$ from the data, we may compare it with the predictions of the statistical theory of nuclear reactions. Consider a compound nucleus C = X + p at an excitation energy E. This nucleus will, if E is high enough, lose energy by emitting particles until its excitation energy is too low for further particle emission (gamma emission from highly excited nuclei is not as improbable as had been formerly supposed,[13] but is still only about 10^{-3} of the reaction cross section[16] and so may be neglected in our discussion). We need to know the binding energies of neutrons and protons to various nuclei, and the level densities; with this information we may use Eq. (9) to calculate the probability that the excited nucleus decays by proton or neutron emission (except for the light elements, to which the statistical theory is not applicable anyway, the probability of alpha or other particle emission is negligible except in special cases).[13] We then can use Eq. (9) again to determine the probability that the residual nucleus is left highly enough excited to emit further particles, and repeat the process.

Tests of the predictions of the statistical theory of nuclear reactions have been made by many experimenters. Partial summaries of their results have been given by Lang and LeCouteur,[17] Cohen,[18] and Blatt and Weisskopf.[13] The most striking success of the compound nucleus was the explanation of resonances in nuclear reactions,[13] and these data alone are sufficient to prove the validity of the concept of a compound nucleus (at least at energies near the binding energies of particles). Lang and LeCouteur showed that a portion of high-energy nuclear reactions may be included within the framework of the theory. On the other hand, it has become increasingly clear that the theory as usually applied does not lead to predictions in accord with the data.[19] The success of the "cloudy crystal ball" model of the nucleus[20] in explaining neutron cross sections at 1 to 3 Mev, and the striking success of the shell model[21] in explaining regularities in nuclear

ground states, tend to contradict the fundamental assumption of the theory that the incident particle amalgamates with the target nucleus to form a highly excited compound nucleus. Thus we might expect that nuclear transparency[22] will be important at energies much lower than previously supposed, and that nucleon-nucleon (or knock-on or direct)[23, 24, 25] reactions will be superposed on the evaporation of particles predicted by the statistical theory.

II. EXPERIMENTAL PROCEDURE

Beam

Protons accelerated to 32 Mev in the linear accelerator were deflected 10^{o} by a steering magnet and passed through a strong-focusing magnetic quadrupole system and into the annex target room (see Fig. 1). The entire path of the beam was in vacuum. A carbon collimator approximately 1 in. thick and 0.75 in. in diameter was placed 4 to 6 ft in front of the target. The targets were placed in a Faraday cup (Fig. 2) in order to measure the total charge. A clip lead from the cup led to a low-leakage Fast condenser, and the voltage across the condenser was measured by a 100% inverse-feedback integrating electrometer; the electrometer output was read on a Speedomax recorder that was calibrated (semiautomatically) against a standard cell before each measurement. The condenser was compared with a secondary condenser that had been calibrated by the National Bureau of Standards to within 0.1%. The electrometer was calibrated against a Leeds and Northrup potentiometer to within 1%, so that the measurement of the voltage across the condenser was accurate to within 1%. The electrometer was carefully checked for drift and grid current before each run, and the rare corrections that were necessary never amounted to more than 1%. No provisions were made for a magnetic field in the cup, but separate tests with and without a field of 400 gauss failed to show any effects of secondary electron emission greater than 0.5% (the measurements were accurate to approximately 2%, and both polyethylene (CH_2) and Pb targets were used). The time constant of the charge-collecting and measuring system was very much greater than the longest bombardment. From this data we concluded that the total charge stopping in the target was determined to within a standard error of 2%.

Proton Energy

The range of the protons was measured on seven occasions. A thin aluminum wedge 3.00 in. long and varying in thickness from 0.121 to 0.223 in. was backed by a 1-by-3-in. nuclear emulsion. The beam

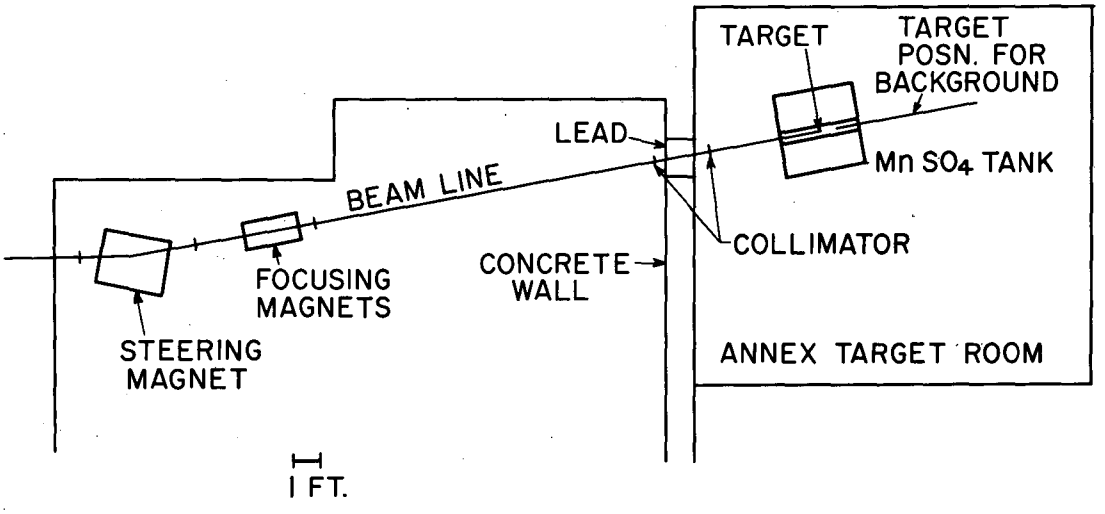

Fig. 1. Schematic diagram of experimental setup.

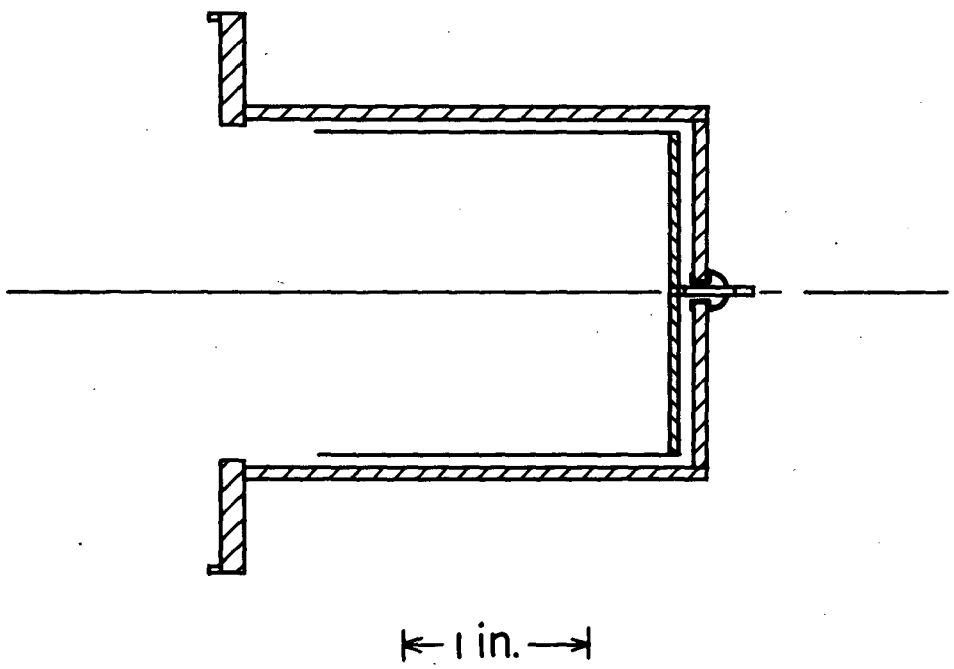

Fig. 2. Schematic diagram of Faraday cup.

passed through the Al wedge and blackened the emulsion; by measuring the distance from one edge of the wedge to the cutoff of the beam pattern, one could determine the range in Al of the protons to within 0.001 in. The ranges varied between 0.196 and 0.190 in., corresponding to energies of 32.6 and 32.0 Mev.[15]

Targets

The targets used were usually 1.5 in. in diameter and were equal to or greater than the range of protons of the appropriate energy,[15] except for the differential targets described below. In cases where metallic targets could not be obtained, or were not convenient to use or form, powdered or liquid targets were used. The liquid target holders had a 0.001-in. stainless steel foil on the front and left a clear area of 1.25 in. The powdered targets were placed in aluminum holders and scotch tape was placed over the front of the holder to hold the powder in place; these holders also provided a clear area of 1.25 in. Three targets (Si, Mn, V) were available only in the form of lumps; these were placed in one of the powdered-target holders with sufficient thickness to make it unlikely that the beam would pass through the target and hit the holder. Na, B, and B^{10} targets were available only in 1-in. diameters. Some elements were bombarded in the form of a compound.

The targets were placed in the Faraday cup and held securely in place with a piece of scotch tape, except for the 1-in. targets, which were held in the center of the Faraday cup by a special holder that screwed into the base of the cup. The Faraday cup was held against the end of the beam pipe by atmospheric pressure; a raised cylindrical lip ensured that the cup was centered to within 1/16 in.

Alignment

Before each day's sequence of bombardments, beam patterns were burned into glass plates and the beam was centered in the beam pipe. A pattern was always taken with a glass plate in the Faraday cup.

The beam was approximately 0.75 in. in diameter and was centered to within 1/16 in. Great care was always taken in this procedure to ensure that none of the beam missed the target.

Neutron Detection

A 3-by-3-ft aluminum tank with a 4.5-in.-diameter tube through the center held the $MnSO_4$ solution. The beam pipe was centered in the tube by a flange that fitted loosely into the tube. A 4-in.-diameter plug, 18 in. long, was filled with $MnSO_4$ solution from the tank and placed in the tank tube in order to intercept neutrons emitted in the forward direction. The plug was filled before, and emptied into the tank at the end of, each bombardment.

The solution was stored in four large tanks placed approximately 200 ft from the target area, and pumps were used to transfer the solution back and forth as needed. The alignment and range measurements were made with the tank empty of solution; when the solution in the tank became too active to be counted accurately, it was pumped back to one of the storage tanks and nonactive solution was pumped into the tank.

Neutrons emitted from the target underwent collisions with hydrogen atoms in the $MnSO_4$ solution and became thermalized.[26] After the neutrons had reached thermal energies, they diffused through the solution until they escaped or were captured by Mn or H (the capture cross sections for S and O are so low that they may be neglected[29]). Those that were captured by Mn formed Mn^{56}, a β- and γ-emitting radioisotope with a half life of 2.59 hours.[28] The distribution of Mn^{56} activity in the tank is, of course, determined by the spatial distribution of thermal and resonance-energy[27] neutrons; thorough mixing of the solution (including that from the plug described above) achieved an integration of the spatial neutron distribution. Following the mixing, a small portion of the solution was drawn from the tank to be counted with immersion Geiger counters.

To guard against sudden counter failures, two separate and nearly identical counter systems were used. The solution to be

counted was placed in a lucite container and the depth adjusted with a syringe. The depth of the solution was chosen so that variations of 1/32 in. caused less than a 1% variation in the counting rate, and the depth could be reproduced to within 1/64 in. Each counter assembly consisted of 5 TGC-5 Tracerlab Geiger counters connected in parallel to a common scaler. The counters could be disconnected individually. A solution of Co^{60} was used before and after each day's run to check the reproducibility of the counters, and to obtain high-voltage plateaus. The general performance of the counters and scalers was satisfactory, and reproducible to within 4% (counting statistics were generally 1%).

The over-all detection efficiency of the tank and counters was determined with the use of a 0.5-g Ra-α-Be source that had been calibrated in December 1954, by the National Bureau of Standards to a standard error of 3%. The date of sealing of the source was unknown, but the growth of Po^{210} in the one-year period following calibration should have been negligible.

The method of calibration assumed that the tank was as efficient in capturing the Ra-α-Be neutrons as it was in capturing neutrons from the target. Measurements of the relaxation length of Ra-α-Be neutrons in water[29] indicate that approximately 98% of them are thermalized in an 18-in. sphere surrounding the source. The great majority of the neutrons emitted from the target probably had energies lower[9, 30] than the mean energy of Ra-α-Be neutrons[31] (approximately 5.5 Mev) and hence were captured more efficiently.

Background

In any attempt to measure neutron yields from high-energy charged particles, the problem of the general neutron background is generally complicated. In our experiment the background was determined by extending the beam pipe so that the target could be placed approximately 2 ft beyond the tank. The target and Faraday cup were positioned and surrounded by approximately 1 ft of paraffin with cadmium sheets on the outside. The yield of neutrons was measured with this arrangement for both CH_2 and Pb targets. From the

measured yields of these targets both in this position and in the tank tube, the background was accurately determined. It amounted to 25% of the lowest yield measured, or about 0.15×10^{10} neutrons per microcoulomb.

Energy Variation

After the yields of 32-Mev protons had been measured, it was decided to reduce the incident beam energy to determine if some of the observed irregularities in the yields were due to the particular incident energy used. Absorbers placed in the beam path would have resulted in a loss of beam intensity and a much more diffuse beam with attendant experimental difficulties. Instead, advantage was taken of the 20-Mev threshold[28] of C^{12} for neutron production by protons and the very low yield from C by 32-Mev protons (see Sec. III). Since C^{12} represents 98.9% of natural carbon, [28] the yield from the C^{13} present is negligible (see Sec. III). The beam energy was degraded by placing a C absorber directly in front of the target in the Faraday cup, and the total yield for 32-Mev protons on C was subtracted as a "background". The absorber was chosen to reduce the beam energy to 18 Mev; the energy had to be lower than the threshold for neutron production in C^{12}, but as high as prudence would allow so that the neutron from the target would be as great a fraction of the total yield (C + target) as possible.

Twenty-three metallic targets were made of such thickness that an incident proton of 32 Mev would be degraded to 18 Mev; these targets were placed in front of a C target in the Faraday cup and the neutron yield measured was that for protons of 18 to 32 Mev in the metallic target. In all cases the yields for the three energy regions were consistent within the experimental error; in fact, the agreement was better than could be expected, indicating that the relative error assigned to the yields was too conservative.

Data Reduction

The data actually measured for each run were (a) the time at which the bombardment ended; (b) the length of the bombardment; (c) the voltage collected across the condenser during the bombardment;

(d) the time at which the counting of the sample began; (e) the length of time of counting; (f) the total number of counts received during the counting interval. In separate measurements a calibrated Ra-α-Be neutron source was placed in the tank (with the Faraday cup and beam pipe in position), and the data listed above were recorded. A sample was taken from the tank before each bombardment to determine the initial Mn^{56} activity. All counting rates were corrected for cosmic-ray background, and a further small correction was made when necessary for background caused by the accelerator.

The counting rates were corrected for dead time, but the rates were restricted so that this correction was never greater than 3%. When the counting rate with all five tubes became too high, the sample was counted with one tube, and the ratio of counting rates between five and one tubes determined each time by counting twice a sample of suitable intensity. The ratio was constant to within 5% and a typical value was 4.9. The ratio was measured at different counting rates a few times to ascertain that it was constant. When the counting rate with one tube became too high, the solution in the tank was replaced with inactive solution.

The samples were counted for times that were short compared with the half life of Mn^{56}, so that the average counting rate was equal to the counting rate at the mid-point of the counting interval. After subtraction of the steady-rate backgrounds (cosmic rays and accelerator), the activity remaining from previous bombardments was subtracted and the net activity at the end of bombardment, A_0, was determined. A_0 was then corrected for the decay that occurred during the bombardment, and

$$A_{00} = A_0 \frac{\lambda t}{1 - e^{-\lambda t}} \qquad (18)$$

was the net counting rate added to the solution as a result of neutrons emitted during the bombardment of t minutes; λ is the decay constant of Mn^{56}. The longest bombardments were less than 10% of the mean life of Mn, ^{56} so we could neglect possible fluctuations in the beam intensity. If A' was the net saturation activity of the solution as the

result of irradiation with a Ra-α-Be source emitting N neutrons per minute, then

$$f = \frac{N}{\lambda A'} \tag{19}$$

was the number of neutrons per unit activity and

$$fA_{00} = \frac{A_{00}}{A'} \frac{N}{\lambda} \tag{20}$$

was the number of neutrons emitted during the bombardment. If V was the voltage collected across the condenser C during the bombardment, then $Q = CV$ was the charge collected by the Faraday cup, and

$$y = f \frac{A_{00}}{Q} = \frac{A_{00}}{A'} \frac{N}{\lambda} \frac{1}{Q} \tag{21}$$

was the yield of neutrons per unit charge.

Errors

Some possible sources of error in the experimental method have been mentioned above. The most serious ones that have not been discussed include variations in the depth of the solution in the tank and insufficient mixing of the solution prior to sampling. Very few neutrons were captured in the outer layers of the solution, and a decrease in the solution level would have resulted in an increase in the specific activity of the solution. The height of the solution was carefully controlled and a limit of 2% may be placed on this source of error. The solution in the main body of the tank was stirred continuously by an electrical stirrer, and after the tank-tube plug had been emptied into the tank, the solution was stirred for 5 min before the sample was drawn out. A test showed that 0 min. delay before sampling gave a net activity 10 ± 1.7% low; 2 min. delay, 1.7 ± 1.7% high, compared with the net activity determined after a 5-min delay.

The measured half life of the $MnSO_4$ solution checked the published value[30] within experimental error.

The value used for the dead time of the counters was that given by the manufacturer (90 μsec) and was checked both by observing the height of the pulses on an oscilloscope as a function of time after a pulse, and by measuring the same yield at very different counting rates.

It was finally decided that the filling, mixing, sampling, and counting procedures were such that a standard error of 2% represented the uncertainty in the gross activity measured for a bombardment. Since the activity of the solution was approximately doubled during each bombardment, the net activity added during a bombardment was determined with a relative (rather than absolute) standard error of approximately 4.5%. This figure was adopted as the standard error of a measurement unless the counting statistical errors were larger.

A comparison of the yields measured for the three different energy regions showed an internal consistency compatible with a much lower relative error. The yields for the 0-to-18- and 18-to-32-Mev energy intervals were added and compared with the yield for the 0-to-32-Mev energy interval measured directly. The percentage deviations were compatible with a standard error of 3%; the yields themselves would then be accurate to approximately 2% on a relative basis.

Neutron absorption by the targets was a possible source of error, but calculations indicated that this amounted to less than 0.5% because of the small size of the targets.

In addition to the relative error quoted above, the absolute values have errors arising from beam monitoring (2%) and neutron-source calibration (taken as 5% to account for both the uncertainty in the source strength and the measurement of the saturation activity). The yield values quoted are then reliable to a standard error of 7% on an absolute basis. In the next section further sources of error that arise in the calculation of σ_{1n} and $\overline{N}$ are discussed.

III. RESULTS

The yield data actually measured are given in Table I in neutrons per μcoulomb (n/μcoul). In all cases an average cross section for the production of one neutron, $\overline{\sigma_{1n}}$, was calculated (see Sec. I):

$$\overline{\sigma_{1n}} = \frac{y}{R}\,\frac{A}{A_0}\;1.60 \times 10^{-13}, \tag{22}$$

where y is the yield in n/μcoul, R is the range of the proton in g/cm^2, A is the atomic or molecular weight,[32] A_0 is Avogadro's number,[33] and 1.60×10^{-13} is the charge of the proton[33] in μcoul. The ranges were taken from the tables of Aron et al.;[15] for elements not given in the tables the ranges were found as follows. The energy loss for a given particle and energy is proportional to $(Z/A)[\log bE + \log (1/Z)]$,[15] so that the range is roughly proportional to $A\,Z^{-1}\,[\log bE + \log (1/Z)]^{-1}$. The ranges given by Aron et al. were multiplied by Z/A and plotted against log Z; a smooth curve resulted (see Fig. 3), and ranges for the other elements could be determined easily. For compounds, ranges were determined by assuming that the stopping power added atomically.[34] Thus for a compound U_mV_n, if dE/dx is in Mev gm^{-1} cm^2, we have

$$\frac{dE}{dx} = \left(\frac{dE}{dx}\right)_U \frac{mA_u}{M} + \left(\frac{dE}{dx}\right)_V \frac{nA_v}{M}, \tag{23}$$

where

$$M = mA_u + nA_v \tag{24}$$

is the molecular weight. The rate of energy loss was found for all elements by plotting (A/Z) (dE/dx) against log Z; a straight line resulted (see Fig. 3) and was used to find dE/dx for elements not given in the tables. For finding the range of a proton in a compound, dE/dx should be found for several energies and integrated: $R = \int_0^E \left(\frac{dE}{dx}\right)^{-1} dE$. Because of the labor involved in this procedure, we instead approximated the ranges in the following manner. The major contribution to R arises from energies near the maximum proton energy, where $(dE/dx)^{-1}$ is greatest, so that an estimate of the range is given by

Table I

Neutron yields for thick targets bombarded by protons
(in 10^{10} neutrons per μcoulomb)

Target	Energy interval of protons		
	0 to 32 Mev	0 to 18 Mev	18 to 32 Mev
Li	9.69	3.16 ± 0.20	
Be	17.7	6.95	*9.46
B	4.21	1.14 ± 0.10	
B^{10}	2.00		
C	0.567 ± 0.037		
Na	3.81	0.51 ± 0.07	
Mg	1.98	0.25 ± 0.08	1.74 ± 0.10
Al	3.16	0.46 ± 0.06	2.64
Si	0.98	0.10 ± 0.06	
P	2.44	0.35 ± 0.06	
S	1.07 ± 0.10	0.008 ± 0.05	
Ti	7.61	1.76 ± 0.13	**7.10
V	9.24	2.30 ± 0.15	
Mn	7.16	1.27 ± 0.11	
Fe	6.00	1.00 ± 0.09	4.78
Ni	3.06	0.32 ± 0.06	2.68
Cu	8.30	1.71 ± 0.12	6.45
Zn	7.16	1.32 ± 0.11	5.85
Se	12.5 ± 0.7		
Zr	11.0	1.67 ± 0.13	8.67
Nb	11.5		
Mo	11.5	2.02 ± 0.13	9.80
Pd	12.4		
Ag	12.2	2.10 ± 0.15	9.65
Cd	12.8	2.14 ± 0.15	10.5
In	12.9	1.98 ± 0.20	11.1
Sn	12.1	1.94 ± 0.19	10.0
Sb	12.7	2.08 ± 0.15	11.0
Te	12.0 ± 0.9		
Ba	12.8		
La	12.5		
Ta	12.6	1.40 ± 0.23	*10.4
W	12.5	1.30 ± 0.19	*10.2
Pt	11.4	1.11 ± 0.10	9.26
Au	10.8	1.05 ± 0.09	9.48
Pb	10.0	0.85 ± 0.09	9.15
Pb^{206}	10.0		
Bi	10.0	0.99 ± 0.10	8.79
Th	20.3	1.94 ± 0.13	16.0
U	23.3	2.28 + 0.15	*18.0
U^{238}	19.5 ± 2.0		
Compounds			
D_2O	5.17	1.23 ± 0.11	
H_2O	0.98 ± 0.06	0.06 ± 0.06	
CH_2	0.392 ± 0.036		
BN	2.92	0.47 ± 0.06	
NaF	3.96	0.72 ± 0.08	
CCl_4	3.34	0.46 ± 0.08	
K_2SO_4	1.19 ± 0.07	0.03 ± 0.05	
KCl	2.70 ± 0.13	0.25 ± 0.06	
CaO	0.569 ± 0.036	0.00 ± 0.03	
Sc_2O_3	4.25 ± 0.28	0.69 ± 0.08	
TiO_2	4.50		
Cr_2O_3	4.60	0.82 ± 0.08	
Co_2O_3	5.69	1.08 ± 0.10	
Ga_2O_3	8.91	1.58 ± 0.22	
GeO_2	7.44	1.31 ± 0.09	
As_2O_3	9.01	1.96 ± 0.13	
NaBr	11.0	1.82 ± 0.13	
$NiBr_2 \cdot 3H_2O$	6.81		
$SrCO_3$	5.59	0.68 ± 0.07	
Y_2O_3	7.2 ± 0.7		
NaI	11.3	2.02 ± 0.13	
CsCl	9.5		
$BaSO_4$	6.60	0.91 ± 0.08	
CeO_2	8.5		
Nd_2O_3	8.5 ± 0.7		
HgO	9.51	0.81 + 0.08	
Bi_2O_3	8.5		

Uncertainties are 4-1/2% except where noted (standard error of a single measurement)
* Target too thin for indicated energy interval.
** Target too thick for indicated energy interval.

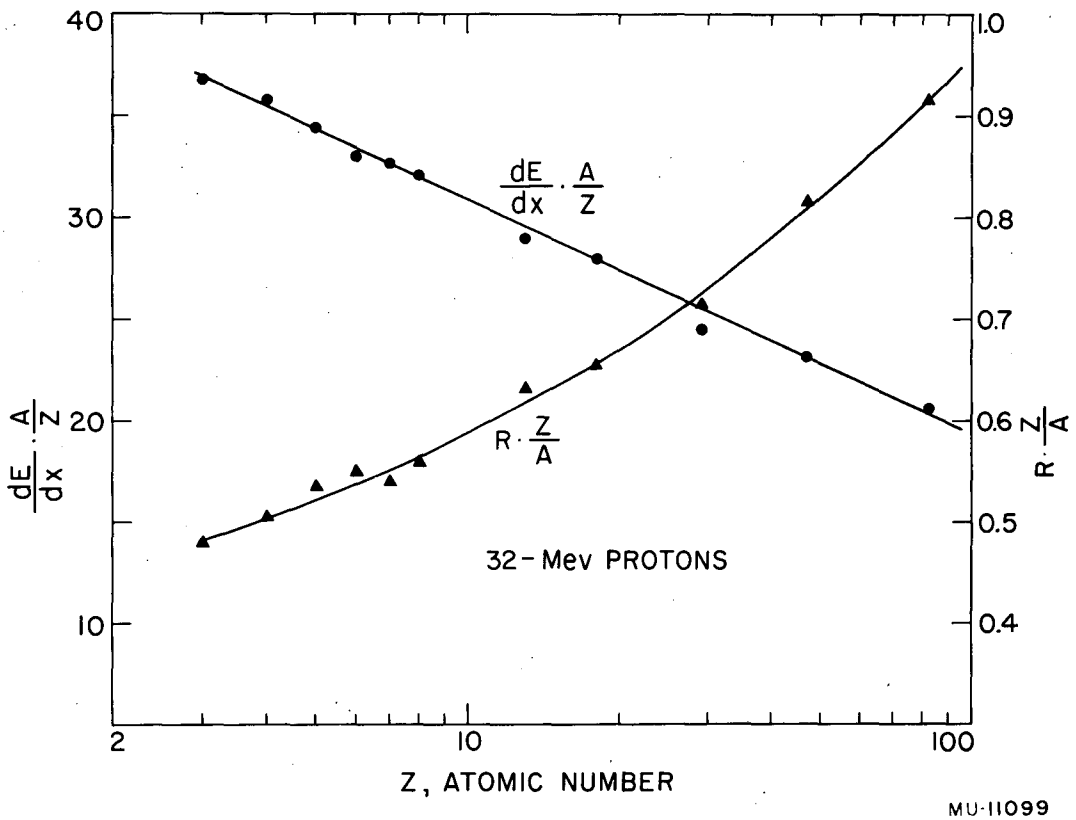

Fig. 3. The straight line is dE/dx for 32-Mev protons multiplied by A/Z, and the curve is range R multiplied by Z/A. The figure (and a similar one for 18-Mev protons) was used to obtain dE/dx and R for elements not given in the Range-Energy Tables.[15] It was also used for compounds with the total charge Z and the molecular weight M replacing Z/A, although this was done only to check other methods of calculating R_{comp}.

$$R_{comp} = R_U \left(\frac{dE}{dx}\right)_{comp} \left(\frac{dE}{dx}\right)_U^{-1} .$$

The relation would be strictly true if $(dE/dx)_U$ were a constant times $(dE/dx)_V$ for all energies. To check the validity of this method, we also calculated ranges of compounds by the following two methods. From the calculated $(dE/dx)_{comp}$ we formed $(dE/dx)M(mZ_U + nZ_V)^{-1}$, and used Fig. 3 to find the corresponding Z_{eff} and $R(mZ_U + nZ_V)M^{-1}$, from which we obtained R_{comp}. Also we plotted dE/dx vs R, and for the calculated $(dE/dx)_{comp}$, found R_{comp}. All three methods agreed within 2%, and so we believe the estimated ranges for compounds are accurate to 3% (standard error). As a further check, we measured $\bar{\sigma}_{1n}$ for a few elements, using both compounds and metallic targets; in all cases the agreement was within experimental uncertainties.

The cross section for a compound is

$$\overline{\sigma_{1n}} = m\overline{\sigma_{1n}}(U) + n\overline{\sigma_{1n}}(V) , \qquad (25)$$

so that if either $\overline{\sigma_{1n}}(U)$ or $\overline{\sigma_{1n}}(V)$ were known, the other could be obtained from the measured $\overline{\sigma_{1n}}$ of the compound.

For targets thick enough to degrade the incident proton energy from 32 to 18 Mev, a cross section averaged over that energy interval was calculated from Eq. (22) with

$$\Delta R = R(32) - R(18) \qquad (26)$$

replacing R.

In cases where only the yields for 32- and 18-Mev protons were measured, the yield for the 32- to-18-Mev energy region was obtained by subtraction and $\overline{\sigma_{1n}}$ was calculated. This procedure is justified by the excellent agreement in the 23 cases where all three yields were directly measured.

Values of $\overline{\sigma_{1n}}$ are given in Table II.

The errors shown in Tables I and II follow the discussion given in Sec. II. The values for 18-Mev protons had larger errors than the other values because they were determined by subtracting the 32-Mev yield for C from the measured quantity, as discussed in Sec. II.

Table II

Cross section for the production of one neutron (in barns)

Element	Energy interval of protons		
	0 to 32 Mev	0 to 18 Mev	18 to 32 Mev
D	0.105 ± 0.007	0.082 ± 0.017	0.119 ± 0.022
Li	0.161	0.148 ± 0.009	0.170 ± 0.014
Be	0.372	0.415	0.339
B	0.108	0.081 ± 0.007	0.122 ± 0.017
B^{10}	0.052		
C	*0.0166 ± 0.009	0	0.047 ± 0.003
N	0.066 ± 0.011	0.00 ± 0.01	0.108 ± 0.023
O	0.0482 ± 0.0030	0.008 ± 0.007	0.0700 ± 0.0060
F	0.170 ± 0.020	0.11 ± 0.02	0.204 ± 0.031
Na	0.187	0.071 ± 0.010	0.249 ± 0.015
Mg	0.103	0.037 ± 0.009	0.140 ± 0.008
Al	0.176	0.074 ± 0.009	0.234 ± 0.012
Si	0.058	0.016 ± 0.010	0.081 ± 0.006
P	0.154	0.062 ± 0.013	0.205 ± 0.037
S	0.071 ± 0.007	0.002 ± 0.013	0.104 ± 0.012
Cl	0.258 ± 0.013	0.10 ± 0.02	0.33 ± 0.02
K	*0.11 ± 0.01	0.00 ± 0.06	0.17 ± 0.02
Ca	0.040 ± 0.006	-0.01 ± 0.03	0.71 ± 0.18
Sc	0.52 ± 0.04	0.25 ± 0.04	0.68 ± 0.07
Ti	*0.640	0.415 ± 0.030	0.80 ± 0.05
V	0.819	0.530 ± 0.036	1.00 ± 0.07
Cr	0.61 ± 0.04	0.32 ± 0.04	0.78 ± 0.06
Mn	0.681	0.332 ± 0.028	0.88 ± 0.06
Fe	0.586	0.266 ± 0.027	0.75
Co	0.82 ± 0.05	0.45 ± 0.05	1.04 ± 0.08
Ni	0.316	0.091 ± 0.017	0.429
Cu	0.879	0.494 ± 0.034	1.07
Zn	0.784	0.394 ± 0.033	1.00
Ga	1.39 ± 0.08	0.72 ± 0.11	1.79 ± 0.13
Ge	1.31 ± 0.07	0.66 ± 0.05	1.73 ± 0.12
As	1.51 ± 0.08	0.91 ± 0.07	1.85 ± 0.14
Se	1.49 ± 0.08		
Br	*1.65 ± 0.09	0.78 ± 0.06	2.30 ± 0.16
Sr	1.38 ± 0.08	0.49 ± 0.05	1.87 ± 0.13
Y	1.29 ± 0.14		
Zr	1.49	0.61 ± 0.09	1.86
Nb	1.58		
Mo	1.63	0.77 ± 0.09	2.20
Pd	1.86		
Ag	1.88	0.87 ± 0.07	2.36
Cd	2.02	0.90 ± 0.06	2.71
In	2.06	0.84 ± 0.05	2.80
Sn	1.95	0.84 ± 0.09	2.57
Sb	2.10	0.91 ± 0.07	2.90
Te	1.99 ± 0.15		
I	2.30 ± 0.13	1.11 ± 0.08	3.01 ± 0.21
Cs	2.07 ± 0.12		
Ba	*2.32	0.93 ± 0.10	3.34 ± 0.22
La	2.24		
Ce	2.11 ± 0.11		
Nd	2.03 ± 0.17		
Ta	2.76	0.80 ± 0.14	3.95
W	2.76	0.75 ± 0.11	3.94
Pt	2.61	0.66 ± 0.06	3.57
Au	2.49	0.63 ± 0.05	3.53
Hg	2.36	0.56 ± 0.06	3.74 ± 0.22
Pb	2.38	0.53 ± 0.05	3.61
Pb^{206}	2.34		
Bi	*2.40	0.62 ± 0.06	3.52
Th	5.18	1.28 ± 0.09	6.54
U	6.05	1.52 ± 0.10	8.10
U^{238}	5.06 ± 0.51		

* Average of two different targets.
Uncertainties are 5% except as noted (standard error of a single measurement).

Unless the yield for 18-Mev protons was large, the subtraction introduced sizable uncertainties in the 18-Mev yields.

The yields and $\overline{\sigma_{1n}}$ were straightforward results of our measurements, but were not susceptible to interpretation. A more fundamental quantity was the average number of neutrons per nuclear interactions, $\overline{N}$. As was pointed out in Sec. I, we needed an average inelastic cross section, $\overline{\sigma_C}$, before we could estimate $\overline{N}$ from $\overline{\sigma_{1n}}$. Inasmuch as any value of $\sigma_C(E)$ was uncertain on the basis of theory, we decided to use the approximation[13] for protons,

$$\sigma_C(E) = \pi(R + \lambda\!\!\!^{-})^2\left(1 - Y\frac{R}{R + \lambda\!\!\!^{-}}\right), \qquad (27)$$

as given in Sec. I. For the nuclear radius R we used $R = 1.5\ A^{1/3} \times 10^{-13}$ and neglected the term $\pi\lambda\!\!\!^{-2}$ in the calculation of $\overline{\sigma_C}$. Eq. (27) gives values approximately 10% higher than those listed in Blatt and Weisskopf[14] for Y = 0.7. Its use for Y > 1 is questionable, for it deviates by a factor of 2 from the more exact calculations; but for values of Y near 1, σ_C is so small that the error introduced in calculating $\overline{\sigma_C}$ in this way is less than the uncertainty in σ_C itself. Recent measurements of (p, n) reaction cross sections[35] at 12 Mev indicated radii near $r_0 = 1.7 \times 10^{-13}$, whereas Kelley's results[36] for 32-Mev protons on Bi gave $r_0 = 1.47 \times 10^{-13}$ and Ghoshal's measurements[37] on Cu gave $r_0 = 1.35 \times 10^{-13}$.

The values of $\overline{\sigma_C}$ used are given in Fig. 4, and the resulting values of $\overline{N}$ in Figs. 5 through 8. Only relative errors based on $\overline{\sigma_{1n}}$ are given for $\overline{N}$, and it is to be understood that the absolute values may be significantly in error because of the uncertainty in $\overline{\sigma_C}$.

Three independent experiments[9, 36, 37] have measured $\sigma_{1n}(E)$ in this energy region. Cohen's results agreed very well with ours throughout the periodic table; Kelley's data gave a $\overline{\sigma_{1n}}$(0 to 32) for Bi of 2.77 compared with the 2.40 ± 0.12 that we measured; Ghoshal's data gave a $\overline{\sigma_{1n}}$(0 to 32) for Cu^{63} of 0.87 compared with the 0.88 ± 0.04 that we measured for natural Cu (70% Cu^{63}).

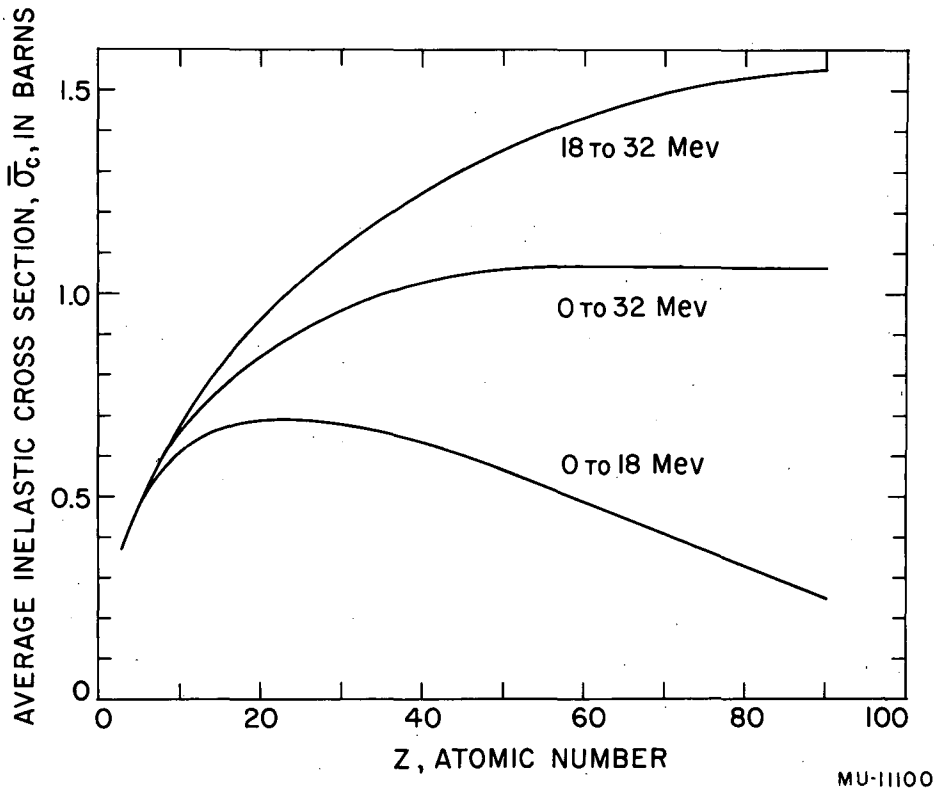

Fig. 4. Cross sections σ_C for the formation of a compound nucleus. Equation (4) was averaged over the energy interval indicated on the figure.

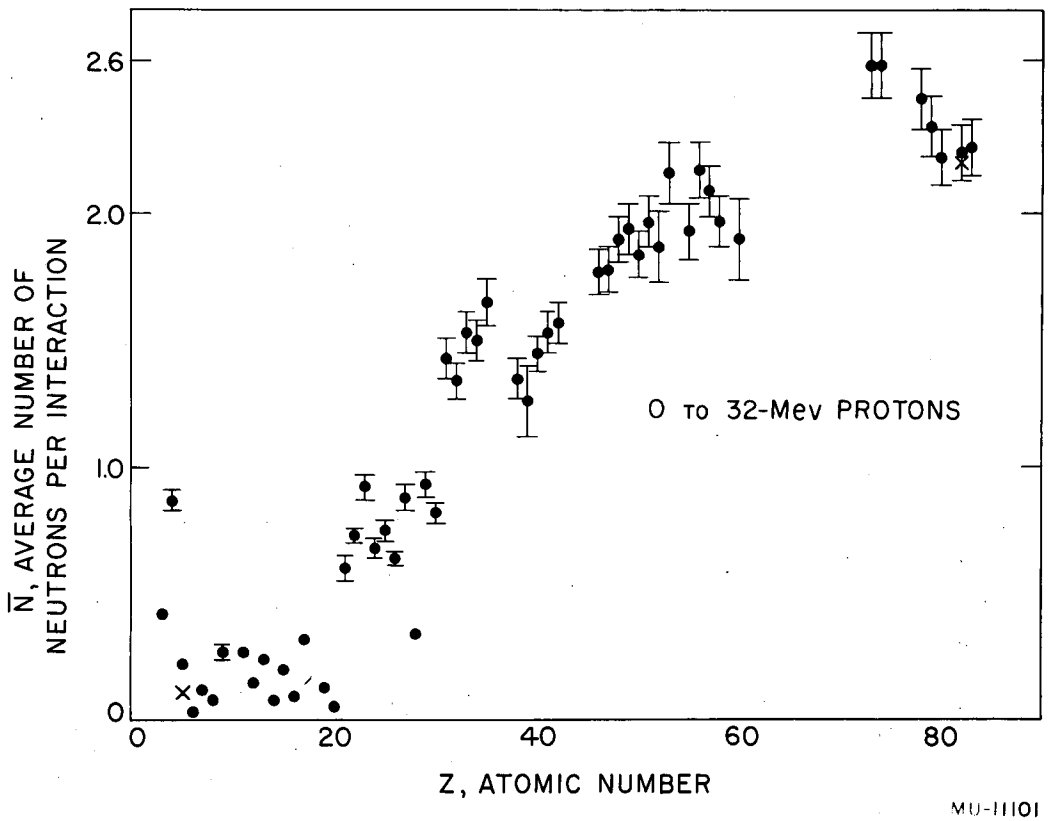

Fig. 5. Average number of neutrons per nuclear interaction $\bar{N}$, plotted against atomic number Z of the target element. Relative errors only are shown and $\bar{N}$ may be in error by an additional 25% because of the approximation of σ_C. The data in this figure are for thick targets bombarded by 32-Mev protons. The crosses are for the B^{10} and Pb^{206} targets. Data for Th and U are not shown.

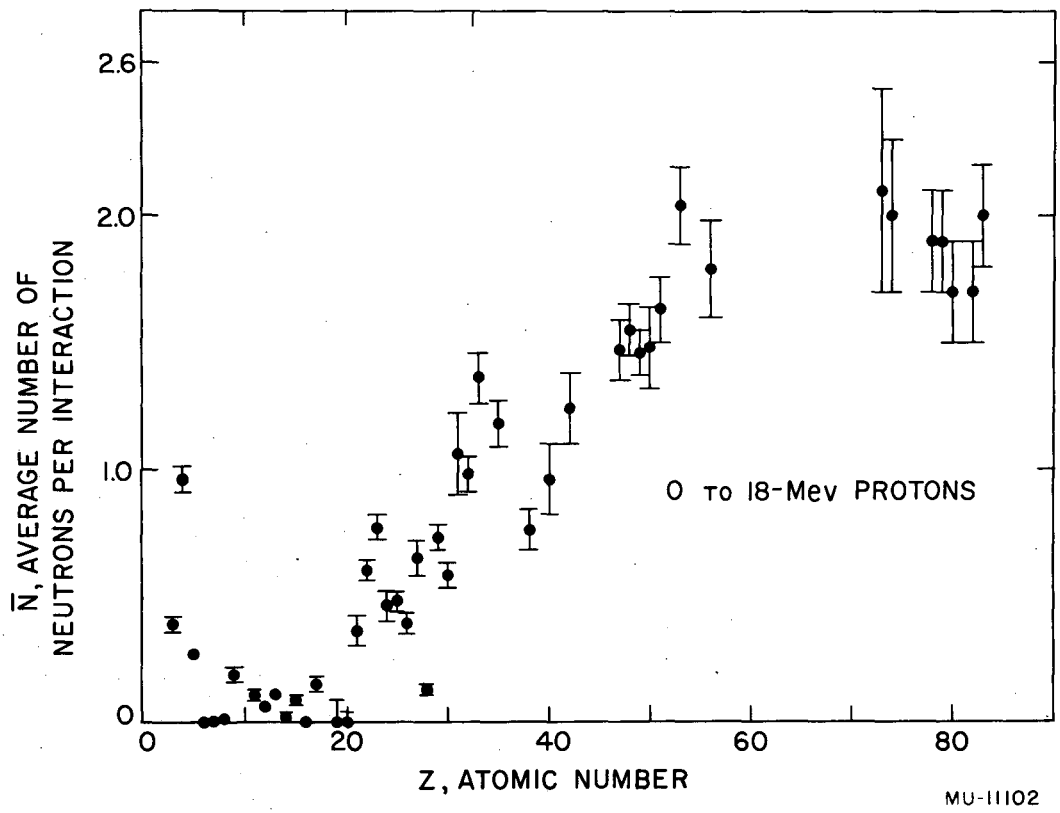

Fig. 6. Data similar to those of Fig. 5 for thick targets bombarded by 18-Mev protons.

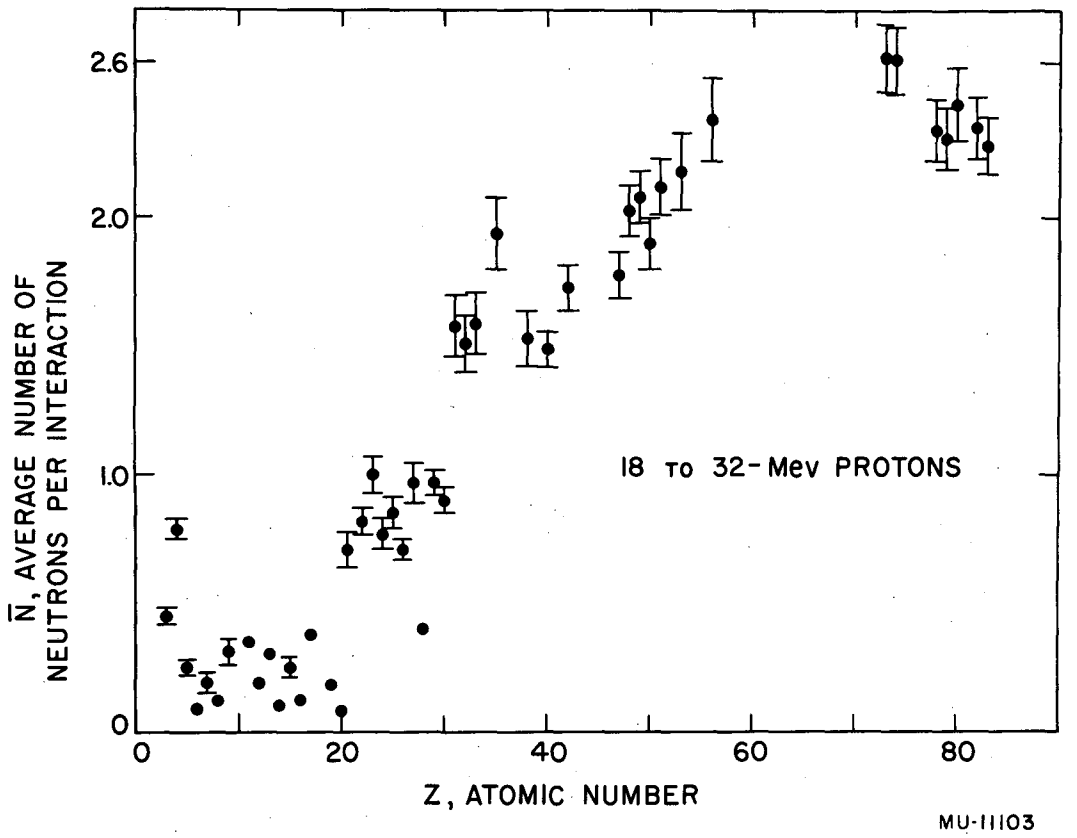

Fig. 7. Data similar to those of Fig. 5 for targets bombarded by 32-Mev protons. The target thickness was chosen to reduce the incident energy to 18 Mev, and some of the data were obtained by subtracting thick-target data for 18- and 32-Mev protons.

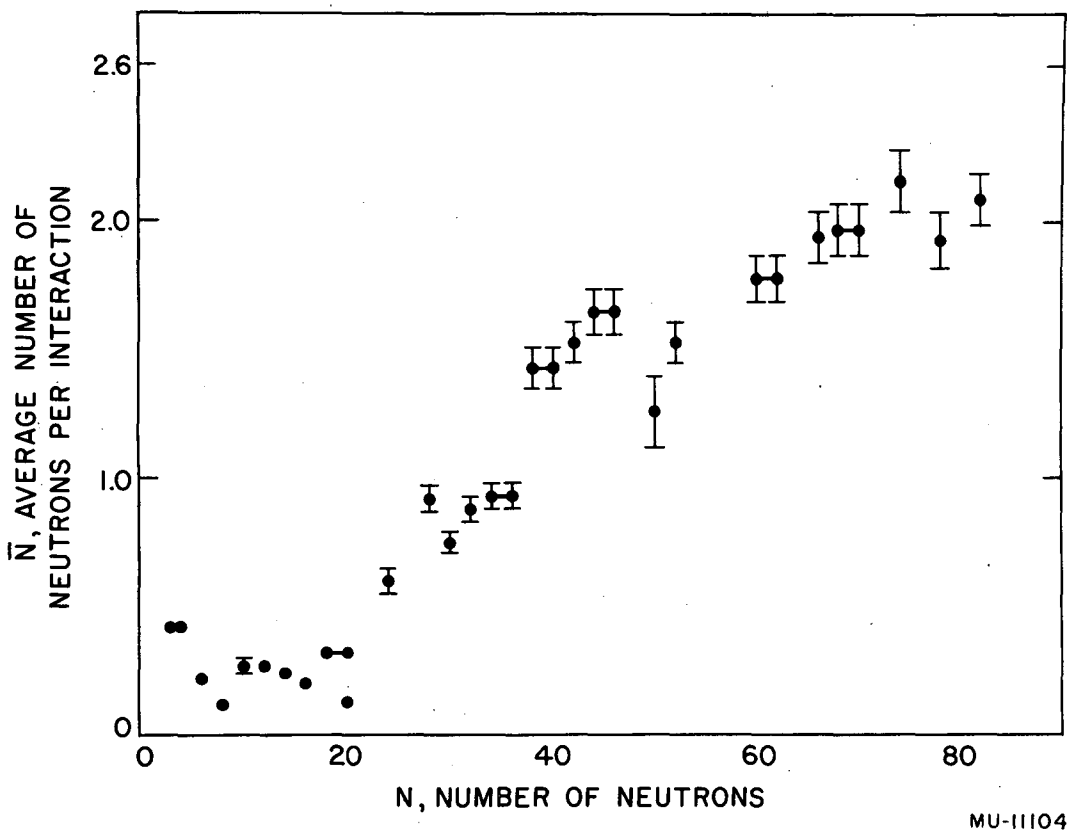

Fig. 8. The data of Fig. 5 plotted against number of neutrons in the target nucleus, N. Only the odd-Z elements are shown, and short horizontal lines join points that represent isotopes of one target element.

IV. DISCUSSION

As we mentioned in the introduction, it is possible to use our data to make a detailed comparison with the statistical theory of nuclear reactions. Before doing so, we wish to point out some of the obvious features of the data.

The most striking features are the discontinuities at Z = 20 and 30, and the very low value of $\overline{N}$ for Ni compared with the neighboring elements. The regular fluctuations in $\overline{N}$ for Z < 30 according to whether the target nucleus is even-even or odd-even are very pronounced.

Two nuclei, D and Be, are worthy of special mention. Aside from the rather unlikely reaction $p + D \rightarrow He^3 + \gamma$, the only inelastic reaction with deuterons that may occur at these energies is the break-up of the deuteron with the emission of one neutron: $p + D \rightarrow 2p + n$. Thus $\overline{\sigma_{1n}}$ closely approximates the total inelastic cross section of D for protons, averaged over the appropriate energy interval.

The behavior of $\overline{\sigma_{1n}}$ for Be is unusual in that it shows a steady decrease with increasing mean energy. From Ref. 6, $\overline{\sigma_{1n}} = 0.51 \pm 0.03$ barns for 12-Mev protons incident on a thick Be target. Taking the mean energy to be the energy of a proton at the mid-point of the range, we find that the value of $\overline{\sigma_{1n}}$ in barns as a function of mean energy is 0.51 ± 0.03 at 8 Mev; 0.42 ± 0.02 at 12 Mev; 0.38 ± 0.02 at 22 Mev; 0.35 ± 0.02 at 26 Mev. The differences in successive values of $\overline{\sigma_{1n}}$ are within the experimental uncertainties, but the regular decrease makes it likely that the effect is a real one.

One reason for such a drop in σ_{1n} would be the slow increase of $R + \lambda\!\!\!^{-}$ with decreasing energy; for an element as light as Be, and in this energy region, $\lambda\!\!\!^{-}$ is of the same order as the nuclear radius R. The increase in the cross section, however, is more than compensated by the effect of the Coulomb barrier. Also, if the increase in $R + \lambda\!\!\!^{-}$ were the sole reason for the increase in σ_{1n}, we should expect Li and perhaps B to show a similar behavior; the data give no such indication, although the differences would not be much larger than the experimental

uncertainties. It may be that the odd neutron in Be spends a large fraction of time outside the nucleus proper, in which case the Coulomb barrier would not reduce the (p,n) cross section as much as the calculations indicate, and the reaction would not proceed through the compound nucleus pattern.

U and Th both have anomalously large values for $\overline{N}$, presumably because fission competes favorably with gamma emission after the residual nuclei are no longer highly enough excited to evaporate neutrons.

The variation of $\overline{N}$ with N, the number of neutrons in the nucleus, does not exhibit any effects much different from those shown in the variation with Z. The fact that the targets were composed of more than one isotope in several cases may have depressed any sharp dependence of $\overline{N}$ on N that cannot be explained by the correlation of N and Z.

In Fig. 9 we have plotted $\theta = (N - Z)/A$ vs Z. The general trend of θ and $\overline{N}$ with Z is very similar, but more striking is the appearance of discontinuities in θ and $\overline{N}$ at Z = 20 and 30, and at Ni. Further, for $Z < 30$, θ reproduces the individual fluctuations in $\overline{N}$. Above Z = 30, θ shows the same trend as $\overline{N}$, but individual fluctuations are no longer matched, and the increase in θ at Z = 30 is not as great as the increase in $\overline{N}$. Such a strong correlation between two quantities cannot easily be ascribed to chance. A good approximation to $\overline{N}$ in terms of θ is $\overline{N} = 25\,\theta^{1.4}$ for the 0-to-32-Mev data.

Cohen and Newman[38] have found a similar break in f_p/f_n at Z = 29. The fact that the break occurs at Z = 29 in their data may be due to their use of a neutron-rich isotope of Zn that had $\theta = 0.12$, appropriate for elements with $Z > 30$. The anomalously low yield for Ni is probably a consequence of the large (p, 2p) cross section of Ni.[39] The difference between $\overline{\sigma_{1n}}$ for 0-to-32-Mev protons for Ni and its neighbors is approximately 150 mb less than the measured (p, 2p) cross section at 21.5 Mev.

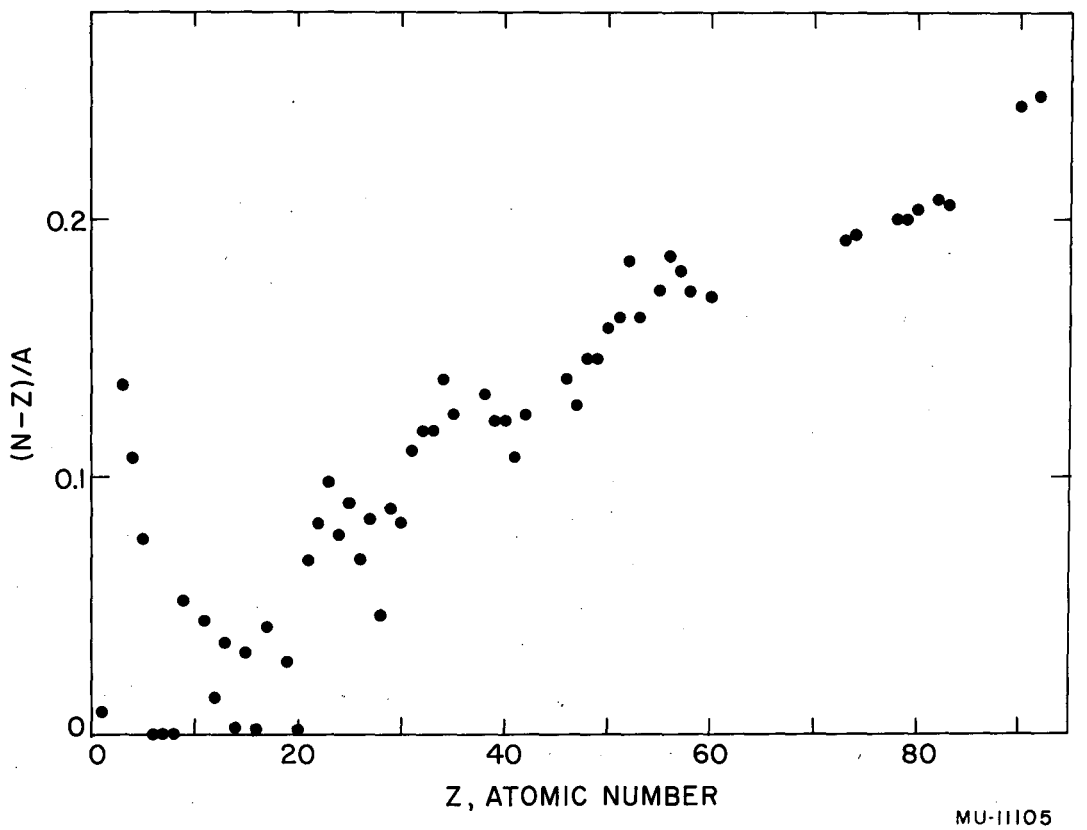

Fig. 9. The average neutron excess per nucleon, $\theta = (N - Z)/A$, plotted against atomic number Z.

In order to make a detailed comparison of our results with the statistical theory of nuclear reactions, we have used the expressions given by LeCouteur.[40] He gives the ratio of the probability of neutron emission to the probability of proton emission as

$$\frac{P_n}{P_p} = \left(\frac{R_n}{R_p}\right)^{1/4}\left(\frac{\Lambda_p}{\Lambda_n}\right)^2 \exp\left(\Lambda_n\sqrt{R_n} - \Lambda_p\sqrt{R_p}\right), \qquad (28)$$

where $\exp(\Lambda^2 E)^{1/2}$ is the energy level density of a nucleus at an excitation energy E. In Eq. (28),

$$\begin{aligned} R_x &= U_a - E_x - V_x', \\ U_a &= \frac{\Lambda^2}{4}\tau^2 \approx \frac{A}{10}\tau^2; \end{aligned} \qquad (29)$$

R_x is the energy available for the emission of particle x from a nucleus a excited to an energy U_a, E_x is the separation energy of x from a, V_x' is the effective potential barrier for x, and τ is the nuclear temperature. For protons we used $V_p' = 0.7\,B$, where B is the Coulomb barrier. Λ_x is the coefficient in the level density expression, for the residual nucleus formed when particle x is emitted from the compound nucleus, and LeCouteur gives

$$\begin{aligned} \Lambda_p &= \Lambda\left(1 + \frac{1.5\theta}{A}\right) \approx \Lambda, \\ \Lambda_n &= \Lambda\left(1 - \frac{1.5\theta}{A}\right) \approx \Lambda, \end{aligned} \qquad (30)$$

LeCouteur's results are based on the Fermi gas model of the nucleus, and the term in θ in Eq. (30) arises from taking into account the difference between N and Z. The terms in front of the exponential in Eq. (28) are nearly unity, so we may take

$$\frac{P_n}{P_p} = \exp\left(\Lambda_n\sqrt{R_n} - \Lambda_p\sqrt{R_p}\right). \qquad (31)$$

A similar expression may be written for P_α/P_p.

The ratios are sensitive to the values of E_x. These were taken from the measured masses[41] and nuclear reaction energies.[42]

Rather than use Eq. (31) to calculate $\bar{N}$, we estimated P_n from our data in the following manner. Consider a nucleus excited enough to emit one, but not two particles. Then $\bar{N} = P_n$. If the nucleus is excited enough to emit two, but not three particles, then

$$\bar{N} = 2P_n(1)P_n(2) + P_n(1)P_p(2) + P_p(1)P_n(2),$$

where the numbers indicate the step in the evaporation process at which the particle is emitted and we have neglected all processes except neutron and proton emission.* If we ignore the change in P_n and P_p during the evaporation, then

$$\bar{N} = 2P_n^2 + 2P_pP_n = 2P_n.$$

Similarly we find $\bar{N} = 3P_n$ if the nucleus is excited enough to emit three particles. The approximations we have made are accurate to approximately 10% on the basis of more complete calculations of P_n for an excitation energy of $(20 + E_p)$ Mev.

We now approximated N(E) as $N(E) = P_n$ for $0 < E < 10$, $2P_n$ for $10 < E < 20$, and $3P_n$ for $20 < E < 30$. Then we calculated $\bar{N} = R^{-1} \int_0^R N(E)dx$ and found $N = 1.70\ P_n$, $2.55\ P_n$, and $3\ P_n$ for the 0-to-18-, 0-to-32-, and 18-to-32-Mev data respectively. The ratios of $\bar{N}$ should then be $\bar{N}(0\text{-}32) = 1.50\ \bar{N}(0\text{-}18)$ and $\bar{N}(18\text{-}32) = 1.18\ N(0\text{-to }32)$; the measured ratios were roughly 1.4 and 1.1, respectively, for $Z \leq 35$.

In Table III we list the values of P_n found from the data for the odd-Z nuclei with $14 < Z < 36$.** We see that $P_n \approx 0.3$ for $Z < 30$, and

---

* These results would not be changed if we included α-emission, but our calculated values of P_n (see below) would be somewhat lower.

** We have considered only the odd-Z nuclei in our calculations because the compound nucleus is then even-even and either proton or neutron emission leads to an odd-even or even-odd nucleus. The variation of level densities[13] between even-even and odd-odd nuclei will not complicate the discussion as it would if the compound nucleus were odd-even.

Table III

Probability of neutron emission, P_n, for odd-Z nuclei ($14 < Z < 36$)

Target	experimental value				calculated ($U = 20 + E_p$)			
	0 to 32 Mev	0 to 18 Mev	18 to 32 Mev	Average	Eq. (31)	Eq. (32)	Eq. (33)	Eq. (34)
P	0.08	0.05	0.08	0.07	0.24	0.24	0.02	0.01
Cl	0.13	0.09	0.13	0.12	0.34	0.23	0.05	0.05
K	0.05	0.00	0.06	0.05	0.13	0.13	0.01	0.01
Sc	0.24	0.21	0.24	0.24	0.67	0.17	0.15	0.10
V	0.36	0.45	0.33	0.38	0.81	0.27	0.30	0.28
Mn	0.29	0.28	0.28	0.28	0.89	0.45	0.45	0.44
Co	0.35	0.38	0.32	0.34	0.89	0.46	0.42	0.38
Cu	0.36	0.43	0.32	0.36	0.70	0.23	0.26	0.23
Ga	0.56	0.62	0.53	0.56	0.80	0.26	0.41	0.46
As	0.60	0.80	0.53	0.64	0.89	0.32	0.56	0.64
Br	0.65	0.69	0.65	0.66	0.90	0.47	0.65	0.73

$P_n \approx 0.6$ for $Z > 30$, in agreement with the results of Cohen and Newman.[38] In column 5 of Table III we have listed the values of P_n calculated from Eq. (31) with $\Delta_n = \Delta_p \sqrt{0.4A}$ for an excitation energy of $(20 + E_p)$ Mev. The break at $Z = 20$ is satisfactorily reproduced, but the calculated values are too high, and do not show the break at $Z = 30$.

LeCouteur's modification of Δ_x indicated in Eq. (30) is too slight to produce a noticeable effect. We may regard the coefficient of θ as a parameter and attempt to force agreement, but in so doing we will lose the theoretical justification. Upon rearranging LeCouteur's expression, we find

$$\frac{P_n}{P_p} = \exp\Delta(1 + 1/2\ y\theta^2)\left[\sqrt{R_n} - \sqrt{R_p} - \frac{2y}{A}\sqrt{R_n}\left(\theta - \frac{1}{A}\right)\right], \quad (32)$$

where θ is calculated in this case for the target nucleus instead of for the compound nucleus, as was the case in Eq. (30). In order to reduce P_n for $Z < 30$ to approximately 0.3 to 0.4, a value of $y = 40$ was needed; but then P_n for $Z > 30$ was also reduced to 0.3. The values of P_n are given in column 6 of Table III.

It is reasonable that P_n/P_p should depend upon θ, or upon some combination of the various θ's for the compound and residual nuclei, although such a dependence might be expected to enter P_n/P_p indirectly by affecting R_x. A direct dependence might be inferred, not only from our data, but also from the observed tendency for proton emission to be favored in proton-induced reactions.[19] For proton-induced reactions, the θ of the compound nucleus will lie below the stable value and proton emission should be favored; of course proton emission is already favored for such reactions because of energy considerations, but as we have seen this effect alone is not sufficient.

We have tried various forms containing θ to attempt to match our results and were moderately successful in reproducing the main features with

$$\frac{P_n}{P_p} = \exp\Delta\left[\sqrt{R_n} - \sqrt{R_p} - 3\,(\theta_p - \theta_c)\,(\sqrt{R_n} + \sqrt{R_p})\right] \quad (33)$$

where θ_p is calculated for the target and θ_c for the compound nucleus. The values of P_n are given in column 7 of Table III. Since $R_n \approx R_p$ in this region, we may use only one of them and double the coefficient of $\theta_p - \theta_c$. The agreement is fair; the break occurs at Z = 32 instead of 30, and the P_n's for Z < 20 are too low. Another expression that gave fair agreement was

$$\Delta_x = \Delta(1 + 4\theta_x). \tag{34}$$

The calculated values are given in column 8 of Table III.

It may be that θ enters into the theory in an indirect manner. There is some evidence[19, 43-47] that the level densities do not increase as fast as the Fermi gas model predicts for low excitation energies, and θ may determine the point in different nuclei at which the level densities start to increase rapidly. Any change in the expression for the level density as a function of energy would, of course, change all the calculated ratios P_n/P_p. Δ depends on the density of protons and neutrons in nuclear matter,[40] or on the radii of their distributions. Recent measurements[48] of nuclear radii have indicated that neutron and proton distributions in nuclei may have different radii; if the ratio of these radii changed discontinuously with θ, Δ_x might be affected enough to reproduce the observed discontinuities.

We also tried to fit the data by assuming that only a few of the nucleons were excited, but the agreement was poor unless we let the number, A', of nucleons that were excited change discontinuously at Z = 30. We needed A' ~ 10 and 25 for Z < 30 and Z > 30, respectively.

It is also quite possible that the statistical theory simply does not apply to the majority of the processes that occur during a nuclear reaction at these energies. Austern et al[23] proposed a type of reaction that is capable of explaining the sharp break in $\overline{N}$ at Z = 30, if a great enough fraction of the reactions proceeded by their mechanism. The simplest case they considered was of a lightly bound neutron in a definite state of orbital angular momentum; an incident proton was supposed to knock out the neutron and be captured into a definite state of orbital angular momentum. Now at Z = 32 the proton added to a nucleus occupies an f shell,[21] so that a proton incident on Ga (Z = 31) might

easily be captured into a state of high angular momentum and knock out a neutron with little or no change in the angular momentum of the residual nucleus. A similar situation occurs at Z = 20, where there are no neutrons available in states of high angular momentum, and the reaction might be suppressed until Sc (Z =21), when neutrons in f states of angular momentum are available. If we assume that this type of reaction gives $\overline{N} = 0.5$, then

$$f \doteq \frac{\overline{N}_{calc} - \overline{N}_{exp}}{\overline{N}_{calc} - 0.50}$$

is the fraction of reactions that proceed by the Austern et al, type. We found f = 0.7 to 0.9 for $20 < Z < 30$, and 0.4 for $30 < Z < 36$.

It is also possible that ordinary knock-on or nucleon-nucleon reactions are very important. Quantitative estimates of the fraction of such reactions have been made[25] for 0-to-30-Mev neutrons on Cu^{63}, and show that the fraction increases from 0 at 13 Mev to 0.3 at 30 Mev. Our data give no clear-cut evidence for such effects, and the discontinuities at Z = 20 and 30 probably could not be completely explained by such reactions.

Direct interactions at the rim of the nucleus have been invoked to explain some data in this energy region.[19, 24] When θ changes abruptly, the excess neutrons are in high angular momentum states and presumably near the edge of the nucleus; thus direct interactions may explain the sharp breaks. If we assume that direct interactions lead to an $\overline{N}$ of 0.25, and use Eq. (31) to calculate $\overline{N}$ for compound nucleus processes, then we have

$$f = \frac{\overline{N}_{calc} - \overline{N}_{exp}}{\overline{N}_{calc} - 0.25}$$

for the fraction of the interactions that are direct. (We assumed that direct interactions led to no excitation of the residual nucleus, so we overestimated f). We found f = 0.7 for $20 < Z < 30$, and 0.3 for $30 < Z < 36$.

We should also point out that recent measurements of inelastic cross sections for 14-Mev neutrons[48, 49] indicated a discontinuity at Z = 20. The cross sections decreased approximately 20% between Ca and Ti instead of increasing slightly. We have neglected this effect in calculating $\overline{N}$, because it would not affect our results appreciably and would tend to emphasize further the discontinuity in $\overline{N}$ at Z = 20, and decrease $\overline{N}$ for Z < 20.

V. SUMMARY AND CONCLUSIONS

From the measured yields of neutrons we have been able to estimate the values of P_n, the probability of neutron emission from an excited nucleus. Three values of P_n for each nucleus agreed very well, indicating that the energy variation of $\overline{N}$ followed the crude estimate we made from the statistical theory. The "measured" values of P_n were much lower than the theory predicted, and showed a discontinuity at Z = 30 that the theory could not reproduce.

A strong correlation of $\overline{N}$ with $\theta = (N - Z)/A$ was noticed, and rough agreement with the data was obtained by introducing an arbitrary dependence of Δ on θ, or an arbitrary dependence of P_n/P_p on $\exp[(\theta_p - \theta_c)\sqrt{R_n}]$.

No conclusions concerning the role of nucleon-nucleon interactions were possible, although it seemed unlikely that such interactions could completely explain the discrepancies.

We have not attempted to make a detailed analysis to calculate individual reactions such as σ(p, pn) for several reasons. Only the statistical theory of nuclear reactions has been developed to the point where detailed calculations are feasible; in any event agreement between calculated reaction cross sections and gross yield values would be of questionable significance. It would be necessary not only to decide the relative importance of compound-nucleus and other processes, but also the relative importance of individual reactions.

The chief value of the data lies in pointing to areas where more detailed information may be sought. The regions near Z = 20 and 30 should be systematically studied to determine the mechanism that is responsible for the abrupt changes in P_n.

A study of individual reactions [38, 39, 50, 51] for elements near Z = 30 would show which ones are most important, and might help to indicate which of the possible non-compound-nucleus reactions are of importance. It is unlikely that much more information could be gained.

A more fruitful direction to follow would be a study of energy and angular distributions of protons, neutrons, and alpha particles from several neighboring elements centered about Z = 30. The theory of Austern et al.[23] predicts definite angular distributions for neutrons on the basis of spin changes, and by fitting observed distributions to predicted ones, it might be possible to decide what fraction of events proceeds through their mechanism. In addition, the statistical theory of nuclear reactions makes definite predictions as to the energy and angular distributions, so that measurements of these might permit assigning a definite fraction of the reactions to compound-nucleus processes. The remaining fraction of the reactions would then have to be explained on the basis of some other type of process, such as nucleon-nucleon or direct interactions.

The more detailed information available from energy and angular distributions of the reaction products might also give clues as to the mechanisms responsible for the sudden change in P_n at Z = 30. A sudden change in the distributions, or in the cross section for a particular distribution (either in energy groups or angular distributions), could be compared with the various theories to determine the types of reactions most likely to account for the change. In particular, it would be interesting to see whether the cross section for proton emission alone changes abruptly at Z = 30, or if the cross section for alpha emission also changes abruptly, and how the ratio P_α/P_p changes. The main interest in studying alpha particles lies in their complex structure; alpha emission almost certainly proceeds through a compound nucleus,[19] so that the behavior of P_α might indicate whether or not the abrupt changes in P_n we observed are caused by compound-nucleus processes.

It would also be of great interest to study neutron-induced reactions for elements near Z = 30 to obtain P_n. These should help to determine the dependence of P_n on θ, and the combinations of the various θ's that are needed. The use of separated isotopes here, and

for proton-induced reactions, would simplify the interpretation of the results. However, a comparison of neutron, proton, and alpha energy and angular distributions offers the best chance of unraveling the various processes that occur at these energies.

ACKNOWLEDGMENTS

I wish to express my appreciation to Dr. Chester M. Van Atta for his constant interest and encouragement, to Professor Burton J. Moyer for his guidance and advice, and to Dr. Yuin-Kwei Tai and Selig N. Kaplan for their major assistance in collecting the data. Dr. Warren Heckrotte was very generous in discussions of the theory, and many of the ideas presented in Sec. IV arose during the numerous discussions with him. Thanks are due to Bob Watt, Wendall Olson, and all members of the operating crew of the linear accelerator for their generous cooperation and assistance in all phases of the experimental work. Particularly I wish to express my debt to Dr. Walter E. Crandall, who taught me most of the techniques used in this work. I must also acknowledge the great debt owed my wife for her patience and understanding.

This work was done under the auspices of the United States Atomic Energy Commission.

REFERENCES

1. J. Chadwick, Nature 129, 312 (1932).
2. See for example Livingston, Henderson, and Lawrence, Phys. Rev. 44, 782 (1933).
3. V. F. Weisskopf, Phys. Rev. 52, 295 (1937); V. F. Weisskopf and D. H. Ewing, Phys. Rev. 57, 472 (1940).
4. L. W. Smith and P. G. Kruger, Phys. Rev. 83, 1137 (1951).
5. Allen, Nechaj, Sun and Jennings, Phys. Rev. 81, 536 (1951).
6. Crandall, Millburn, and Schecter, "Neutron Yields from Thick Targets Bombarded by 24-Mev Deuterons and 12-Mev Protons, "UCRL-3177, Oct. 1955.
7. W. E. Crandall et al., UCRL-2063, Jan. 1953; 2705, Sept. 1954; 2706, Sept. 1954.
8. W. W. Havens et al., unpublished data.
9. B. L. Cohen, Phys. Rev. 98, 49 (1955).
10. L. W. Alvarez et al., Rev. Sci. Instr. 26, 111 (1955).
11. We are indebted to the National Bureau of Standards and particularly to Dr. J. A. De Juren for comparing our source with their Ra-γ-Be standard source.
12. N. Bohr, Nature 137, 344 (1936).
13. J. M. Blatt and V. F. Weisskopf, Theoretical Nuclear Physics, New York, Wiley 1952.
14. Ref. 13, p. 350.
15. Aron, Hoffman, and Williams, "Range-Energy Curves, " AECU-663.
16. B. L. Cohen, Phys. Rev. 100, 206 (1955).
17. J. M. B. Lang and K. J. LeCouteur, Proc. Phys. Soc. A67, 586 (1954).
18. B. L. Cohen, Phys. Rev. 92, 1245 (1953).
19. Brookhaven Conference on Statistical Aspects of the Nucleus, BNL-331.
20. Feshbach, Porter, and Weisskopf, Phys. Rev. 96, 448 (1954).

21. M. G. Mayer and J. H. D. Jensen, Elementary Theory of Nuclear Shell Structure, New York, Wiley 1955.
22. R. Serber, Phys. Rev. 72, 1114 (1947).
23. Austern, Butler, and McManus, Phys. Rev. 92, 350 (1953).
24. R. M. Eisberg and G. Igo, Phys. Rev. 93, 1039 (1954).
25. R. Nakasima and K. Kikuchi, Progr. Theor. Phys. 14, 126 (1955).
26. E. Amaldi and E. Fermi, Phys. Rev. 50, 899 (1936); Amaldi, Hafstad, and Tuve, Phys. Rev. 51, 896 (1937).
27. "Neutron Cross Sections," AECU-2040.
28. Hollander, Perlman, and Seaborg, Revs. Modern Phys. 25, 469 (1953).
29. J. H. Rush, Phys. Rev. 73, 271 (1948).
30. P. C. Gugelot, Phys. Rev. 81, 51 (1951).
31. H. L. Anderson, Preliminary Report No. 3, Nuclear Science Series, National Research Council, 1948.
32. Handbook of Chemistry and Physics, 33rd Ed., Chemical Rubber Publishing Co., Cleveland, Ohio, 1951.
33. J. W. M. DuMond and E. R. Cohen, Revs. Modern Phys. 25, 706 (1953).
34. T. J. Thomson "Effect of Chemical Structure on Stopping Powers for High-Energy Protons" (Thesis), UCRL-1910, Aug. 1952.
35. H. G. Blosser and T. H. Handley, Phys. Rev. 100, 1340 (1955).
36. Elmer L. Kelly, "Excitation Functions of Bismuth," UCRL-1044, Dec. 1950.
37. S. N. Ghoshal, Phys. Rev. 80, 989 (1950).
38. B. L. Cohen and E. Newman, Phys. Rev. 99, 718 (1955).
39. Cohen, Newman, and Handley, Phys. Rev. 99, 723 (1955).
40. K. J. LeCouteur, Proc. Phys. Soc. A63, 259 (1950); A65, 718 (1952).
41. Atomic masses were taken from Collins, Nier, and Johnson, Phys. Rev. 84, 717 (1951); 86, 408 (1952); 94, 398 (1954), and from B. G. Hogg and H. E. Duckworth, Can. J. Phys. 31, 942 (1953); 32, 65 (1954).

42. Reaction energies were taken from R. W. King, Revs. Modern Phys. 26, 327 (1954); and C. W. Li, Phys. Rev. 88, 1038 (1952).
43. Hughes, Garth, and Levin, Phys. Rev. 91, 1425 (1953).
44. Feld, Feshbach, Goldberger, Goldstein, and Weisskopf, NYO-636.
45. H. A. Bethe and H. Hurwitz, Jr., Phys. Rev., 81, 898 (1951).
46. D. B. Beard, Phys. Rev. 94, 738 (1954).
47. P. C. Gugelot, Phys. Rev. 93, 425 (1954).
48. W. N. Hess and B. J. Moyer, Phys. Rev. 101, 337 (1956).
49. E. R. Graves and R. W. Davis, Phys. Rev. 97, 1205 (1955).
50. Cohen, Newman, Charpie, and Handley, Phys. Rev. 94, 620 (1954).
51. B. L. Cohen, Phys. Rev. 100, 206 (1955).